Study of Deposition Temperature on Properties of Aged Nanostructured Nickel Oxide for Solar Cells

Ukoba, O. Kingsley*‡, Inambao, L. Freddie**, Eloka-Eboka, C. Andrew***

*‡Department of Mechanical Engineering, University of KwaZulu-Natal, Durban, 4041, South Africa.

** Department of Mechanical Engineering, University of KwaZulu-Natal, Durban, 4041, South Africa.

*** Department of Mechanical Engineering, University of KwaZulu-Natal, Durban, 4041, South Africa.

(ukobaking@yahoo.com, inambaof@ukzn.ac.za, fatherfounder@yahoo.com)

‡
Corresponding Author; Tel: +27640827616, +2348035431913

Received: 16.10.2017 Accepted:27.02.2018

Abstract- Nanostructured nickel oxide (NiO) films were deposited on preheated glass substrate using spray pyrolysis technique. This study examined the influence of deposition temperature on properties of aged nickel oxide thin films. A preferred orientation along the (1 1 1) plane was observed with a polycrystalline cubic structure. Films were formed with a stoichiometric ratio at higher deposition temperatures. It was revealed that the surface morphology and elemental composition of NiO films can be optimized by deposition temperature. The optical band gap grew as deposition temperature increased. Refractive index decreased with increasing deposition temperature. Optical band gap varied from 3.31 eV to 3.69 eV as deposition temperature increased. The deposition temperature has an influence on properties of aged NiO films. These results may be of interest in the development of affordable and efficient solar cell fabrication especially in developing countries.

Keywords- NiO; solar cell material; deposition temperature, developing countries, aged.

1. Introduction

Provision of affordable and efficient energy is a major human challenge [1]. Electricity is nonexistent for 20 % of the world's population with developing countries comprising 99.8 % of that figure [2]. Several developing countries lack access to electricity [3] while many others have highly disrupted supply with less than four hours of power supply per day [4]. Optimized techniques and materials are being researched to solve this energy problem. Interest is on development of renewable energy due to their vast advantage [5-7]. Energy from the sun has been proposed as a viable solution for power supply [8-9]. Photovoltaic is one way of using the solar energy [10-14]. Solar energy can be converted to useful direct current electricity using solar cells [15]. The focus of current solar cell research is on affordability and efficiency. Most of the equipment used for thin film deposition is expensive [16] and vacuum-based [17]. This has caused researchers in developing countries look for in-country resources, resulting in research on inexpensive materials and methods requiring only a small power supply.

Nanostructure metal oxides are reported to offer improvement for solar cells [18]. Nickel oxide (NiO) is a unique metal oxide with several uses [19-24]. It is a p-type metal oxide and is an inexpensive material. It can be manufactured by several techniques such as sputtering [25], sol-gel [26], laser ablation [27], electron beam deposition [28] and chemical bath deposition [29]. Studies have been conducted on the effect of ageing and the effect of deposition temperature on NiO films [30-32], showing that ageing and deposition temperature improved NiO film properties. However, most of the studies focused on the influence of substrate temperature on sensing properties, electrochromic properties [33] and photovoltaic cells [34]. There is little or no systematic study of the influence of deposition temperature on aged NiO film properties. Therefore, there is a need to study their combined effect on NiO films.

This research will help to ascertain if deposition of nickel oxide at either low temperatures or temperatures above 350 ^{o}C give the same optimal properties. This temperature was reported to be the optimal range for pyrotic decomposition of NiO [35]. Therefore, this research will study the influence of deposition temperature below 350 ^{o}C and above 350 ^{o}C on properties of aged NiO films. Morphological, structural, elemental, and optical properties will be examined with a view to optimizing NiO film for efficient and affordable solar cells application.

2. Experimental Procedure

2.1 Deposition

Pure nickel (II) acetate tetrahydrate $Ni(CH_3CO_2)_2.4H_2O$ of 0.05 M was mixed and stirred in 50 mL distilled water. The solution was left for one week after mixing to age before deposition. This was spray deposited using the set-up in Fig. 1. Thereafter, it was deposited at different temperatures T_d (< 350 ºC and ≥ 350 ºC). The samples were sprayed from 270 ºC to 325 ºC for Td< 350 ºC samples and done at 350 ºC to 400 ºC for Td ≥ 350 ºC. The glass substrate was chemically and ultrasonically cleaned before usage for deposition of the solution. Other deposition parameters were maintained to obtain uniform film thickness.

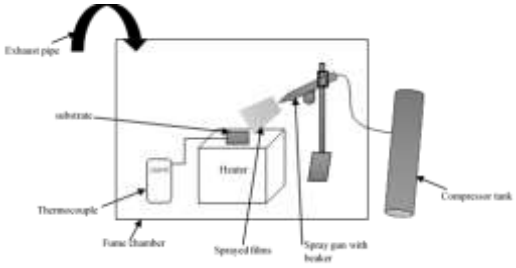

Fig. 1. Experimental set-up of Spray pyrolysis technique.

The optimum deposition parameters of spray deposited NiO films are shown in Table 1. Each droplet was found to be smaller than micro sized particles. The sprayed solution on the preheated substrate glass experiences evaporation and solute precipitation before pyrolytic decomposition as shown in equation (1). Nickel oxide was obtained as a final product [36].

$$Ni(CH_3COO)_2.4H_2O \xrightarrow{heat} NiO + 7H_2O \uparrow + 4CO_2 \uparrow \quad (1)$$

The colour of prepared thin films was observed to be gray, uniform and strongly adherent to the glass.

Table 1. Optimum deposition parameter of SPT NiO film.

Deposition parameter	Value
Height of spraying nozzle to substrate distance	20 cm
Spray rate	1 ml/min
Spray time	1 min
Time between sprays	30 sec
Carrier gas	Filled compressed air of 1 bar

2.2 Characterization

The morphology of deposited NiO film was studied using Scanning Electron Microscope ZEISS EVO MA15VP. An Energy Dispersive X-ray Spectrometer (EDS or EDX: "GENESIS XM2") was used for elemental composition. An EMPYREAN (PANalytical) X-ray powder diffractometer model was used for structural properties of deposited NiO films from 5 º to 90 º 2θ angles. The absorption of the film was measured with a Perkin Elmer Spectrum 100 Fourier Transform Infrared Spectrometer (FTIR). The measured film thickness was compared with the calculated values obtained using the weight difference method. Optical properties were studied in wavelengths of 300 nm to 1000 nm with a SHIMADZU UV-3600UV-VIS Spectrometer.

3. Results and Discussion

3.1 Morphological studies

SEM micrographs are represented in Fig. 2. These micrographs reveal homogeneous, smooth, well adherent films devoid of pinholes and cracks. The film of $T_d \geq 350$ ºC has better distribution of grains than $T_d < 350$ ºC, although it has almost the same particle size and shape as $T_d < 350$ºC. This may be ascribed to the ageing of the films and optimized deposition parameters. This shows that deposition temperature influences structural properties of aged NiO films by increasing grain on the film. These micrographs are an improvement on earlier results reported by Chen et al. [37] using radio-frequency (RF) magnetron sputtering.

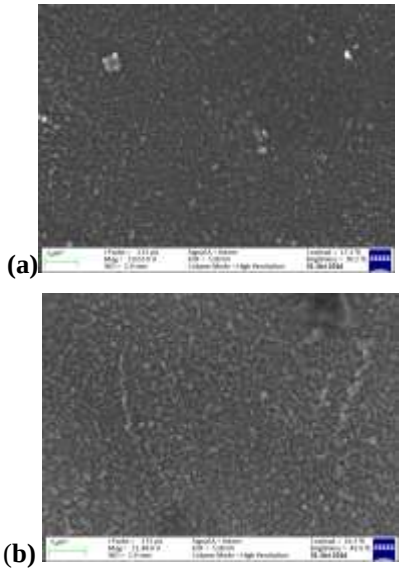

Fig. 2. SEM micrographs of aged (one week) nickel oxide (NiO) film on glass substrate at (a) Td < 350 ºC and (b) Td ≥ 350 ºC

3.2 Elemental composition analysis

Fig. 3 shows the EDX for the different deposition temperatures for NiO thin films. Both spectra confirm presence of Ni and O elements in NiO thin films. Oxygen concentration in deposited NiO films decreases as deposition temperature increases. This may be due to increased film growth on the glass substrate as seen from Fig. 2 thereby making less of the glass (oxygen) visible.

Related results were reported by Lu et al. [38]. An additional Si element was also observed from the EDX. This is because Silicon (Si) is a major material in the soda-lime glass substrate used [39].

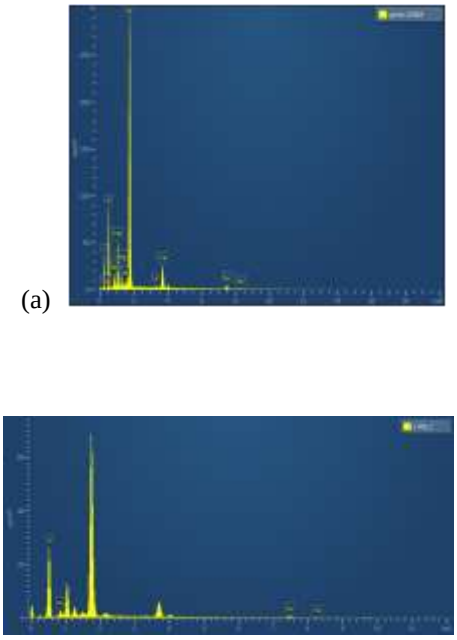

Fig. 3. EDX spectra for one week aged nickel oxide (NiO) film on glass substrate at (a) Td < 350 ºC and (b) Td ≥ 350 ºC

3.3 Structural studies

The phase and preferred orientation of deposited nanostructured NiO films was determined using an x-ray diffractometer. Fig. 4 gives XRD patterns of deposited nanostructured NiO films at Td < 350 ºC and Td ≥3 50 ºC.

The peak diffraction for Td < 350 ºC is at (2θ = 43.36º and 50.54º) for the (1 1 1) and (2 0 0) planes respectively. At Td ≥ 350 ºC, peak diffraction is (2θ = 36.96º and 43.14º) for the (1 1 1) and (2 0 0) planes respectively. The XRD analysis confirms Bunsenite which correspond to JCPDS card: 04- 0835 for NiO [40]. A high intensity was recorded for $T_d \geq 350$ ºC in both planes, which may be due to better alignment of the grains. This led to increased grain growth at higher deposition temperature. It can also be ascribed to increased crystallinity as deposition temperature increased. This is related to the reported value of 37.3º for the (1 1 1) plane by Sharma et al. [30].

The XRD spectra shows that films prepared at T_d < 350 ºC have weak and broadened (1 1 1) diffraction peaks, which implies poor crystallinity. However, those at $T_d \geq 350$ ºC have good crystallinity and the (1 1 1) preferred orientation. These are pointers that the microstructure of NiO films are influenced by deposition temperature as evidence from the grain growth at higher deposition temperature. NiO films with either a (1 1 1) or (2 0 0) preferred orientation are recommended for optoelectronic applications [41].

There is separate colliding of Ni^{2+} and O^{2-} on the growing aged NiO films surface at lower deposition temperature, thereby making it difficult for Ni^{2+} and O^{2-} to recombine due to insufficient energy or oxygen. There is a tendency for non-stoichiometric ratio films to be formed which are electrostatically polar. Ni^{2+} and O^{2-} strike, simultaneously, on the growing aged NiO films at higher deposition temperature, producing film formation with stoichiometric ratios that are electrostatically neutral [42]. This is corroborated with a higher intensity for the (1 1 1) preferential orientation for low deposition temperature [43].

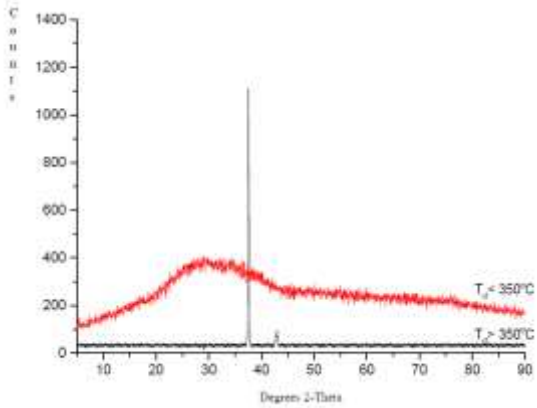

Fig. 4. XRD patterns of one week aged nanostructured NiO films at different deposition temperature

The Debye-Scherer relationship [44]; [45] in equation (2) was used to obtain the average crystallite size.

$$D = \frac{k\lambda}{\beta \cos \theta} \quad (2)$$

Where B represents the Full Width at Half Maximum (FWHM) peak intensity (in Radian), λ denotes wavelength, θ represent Bragg's diffraction angle and k is 0.89.

Other structural parameters are shown in Table 2.

Table 2. Parameters from XRD data

Deposition Temperature	hkl	Diffraction angle 2theta	FWHM	Relative intensity	d-spacing
T_d < 350 ºC	(1 1 1)	43.3641	0.5038	100	2.42290
	(2 0 0)	50.5425	0.7557	81.78	2.09685
$T_d \geq 350$ ºC	(1 1 1)	36.9621	0.5510	62.14	2.43190
	(2 0 0)	43.1404	0.3149	100	2.09688

The average crystallite size of NiO film index for the (1 1

1) and (2 0 0) planes for $T_d \geq 350$ °C as observed from XRD are 26 nm and 47 nm respectively. Those of $T_d < 350$ °C are 34 nm and 23 nm for the (1 1 1) and (2 0 0) planes respectively.

3.4 Optical properties

The film thickness was considered for the NiO films at deposition temperatures below ($T_d < 350$ °C) and above ($T_d \geq 350$ °C). The measured data is depicted in Fig. 6. This was compared with the calculated value. The calculated value was obtained using the weight difference method expressed in Equation (3) [46]:

$$t = \frac{m}{A\rho} \tag{3}$$

Where t denotes film thickness, m represents the actual mass deposited, A denotes thin film area while ρ represents the density of material.

Fig. 7 shows the calculated values. Both measured and calculated values are in good agreement. Film thickness grew as deposition temperature increased. The NiO film thickness was controlled by keeping deposition parameters constant. NiO thin film average thickness was between 11.85 µm and 12.55 µm.

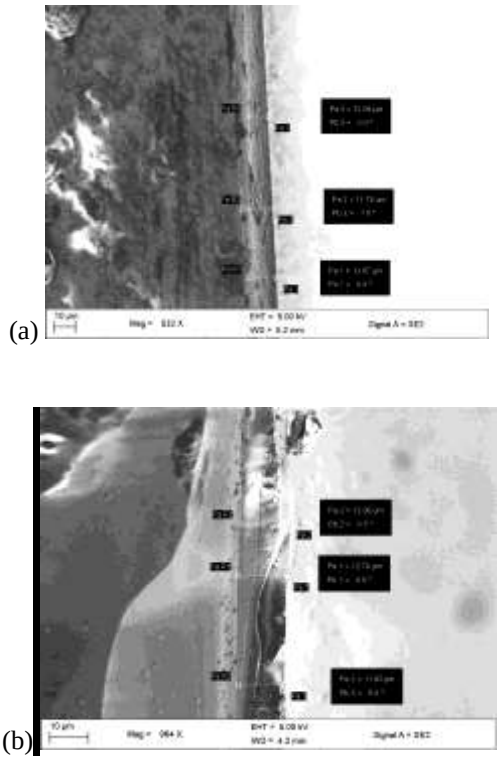

Fig. 6. Measured film thickness for aged (one week) nickel oxide (NiO) film on glass substrate at (a) $T_d < 350$ °C and (b) $Td \geq 350$ °C

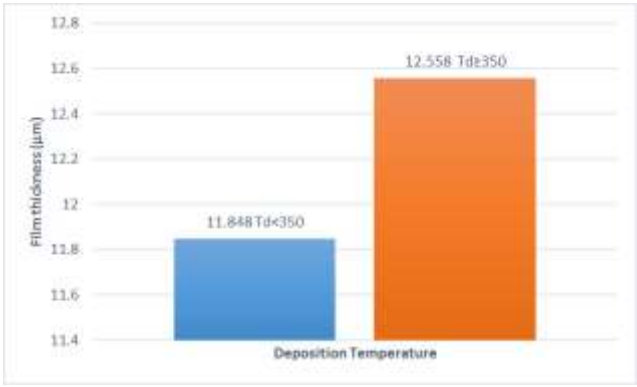

Fig. 7. Calculated film thickness of the aged (one week) NiO films at different deposition temperature.

Fig. 8 gives FTIR spectra used to identify molecular components and the structure of NiO films. It gives the spectrum of aged (one week) 0.05 M NiO films at $T_d \geq 350$ °C alone, in the range of 400 cm^{-1} and 4000 cm^{-1}. The NiO stretching vibration mode was recorded in the broad absorption band region of 432 cm^{-1} to 698 cm^{-1}. This is similar to the earlier reported NiO absorption range [47]. The broadness confirms that the NiO are nanocrystalline. The NiO film FTIR absorption is blue-shifted due to their nanostructure size. Other significant absorption bands were also recorded. The band at 3475 cm^{-1} reveals an O-H (hydroxyl group or hydroxide ion) stretching vibration. This is the natural portion of water due to a self-ionization reaction [48]. An H-O-H bending vibration mode was observed at 1630 cm^{-1}. This shows that there is a negligible quantity of water in the NiO film. This may be attributed to adsorption of water from the air since the experiment was conducted in open air [49]. This is corroborated by the EDX result in Fig 3. The region between 1000 cm^{-1} to 1500 cm^{-1} with band centre at 1210 is assigned O-C=O symmetric and non-symmetric stretching vibration. This accounts for the traces of H_2O and CO_2 in the reaction of Equation (1) which were burnt off. There is no band indicating the presence of other groups, confirming that there is no impurity in the film and that the sample was washed and well cleaned. This result agrees with the standard FTIR data for NiO films as reported by [50]. The NiO film deposited at $T_d < 350$ °C did not give FTIR. This may be due to non-absorption of the film.

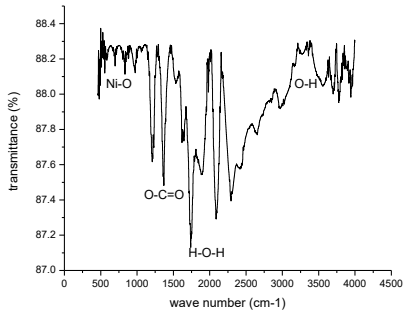

Fig. 8. FTIR spectrum of aged (one week) 0.05 M NiO films at $T_d \geq 350$ °C.

Fig. 9 represents measurement of transmittance and wavelength for deposited NiO films at the deposition temperatures. Transmittance grew from 70.70 % to 76.41 % as deposition temperature increased. However, both films exhibited high transparency in visible and near IR regions. This occurred at wavelengths of 1000 nm and 611 nm respectively. This may be due to an increase in film thickness and absorbance (shown in Fig. 10) as deposition temperature increases, making the scattered radiation more pronounced because of surface roughness [51]. These results exceed previously reported values of less than 70 % by Ismail et al. [52].

Absorption coefficient, α was obtained using Equation (4) [53]:

$$\alpha = (2.303 \times A) / t \quad (4)$$

Where t is film thickness and A is absorbance. The relationship between optical absorption and optical energy band gap is expressed in Equation (5) [54]; [55]:

$$\alpha^2 = C(h\upsilon - E_g) \quad (5)$$

Where C has constant value, h denotes Planck's constant, υ represent incidence light frequency, and E_g denotes optical energy band gap.

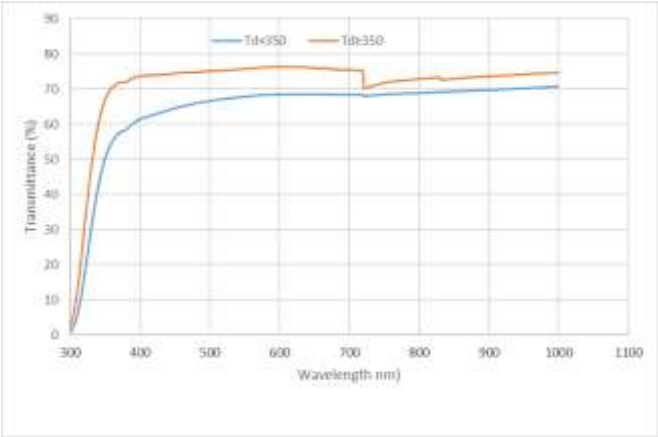

Fig. 9. Plot of transmittance against wavelength of deposition temperature of NiO films

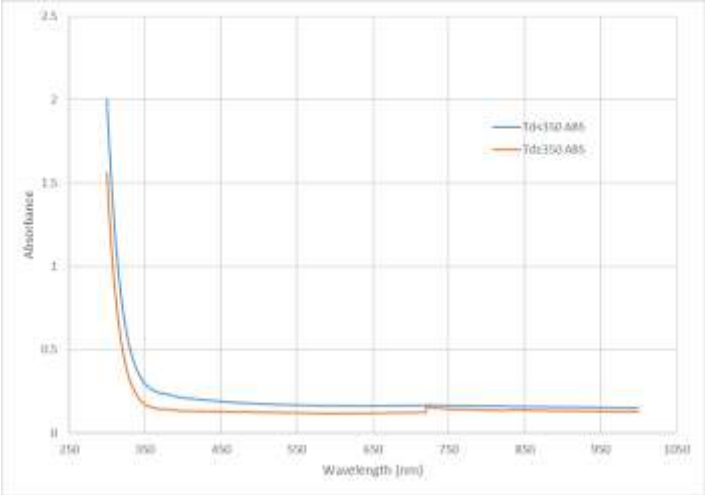

Fig. 10. Plot of absorbance against wavelength of deposition temperature of NiO films

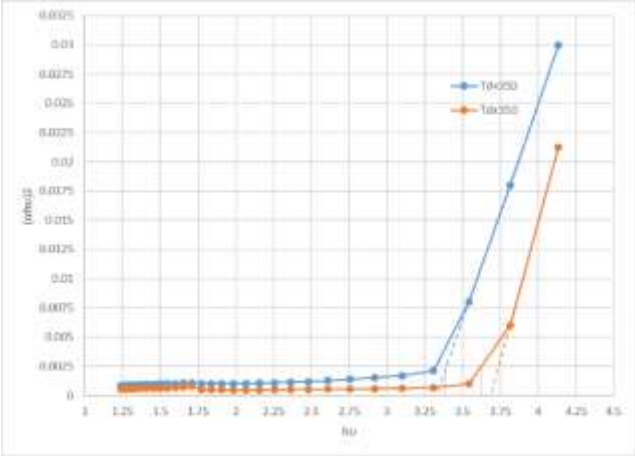

Fig. 11. Graph of $(\alpha h\upsilon)^2$ against hυ for NiO films

Fig. 11 shows a graph of $(\alpha h\upsilon)^2$ against hυ for aged NiO films spray deposited at both deposition temperatures. Extrapolation of Fig. 11 to hυ axis for $(\alpha h\upsilon)^2 = 0$ gives the optical band gap. A decrease in slope of the plot is observed as deposition temperature increases. A shift towards lower energy is observed for value optical band gap. The reduction is attributed to the Moss-Burstein shift [56, 57]. Optical energy band gaps are 3.31 eV and 3.69 eV for T_d <350 ºC and $T_d \geq 350$ ºC respectively. This gives a better optical band gap compared to the existing reported value of 3.5 eV [58]. This may be ascribed to crystallite size increment [59]. The quantum size effect may be responsible for the large value of the band gap of NiO films [60]. Careful and well optimized deposition parameters also help in obtaining a better optical band gap.

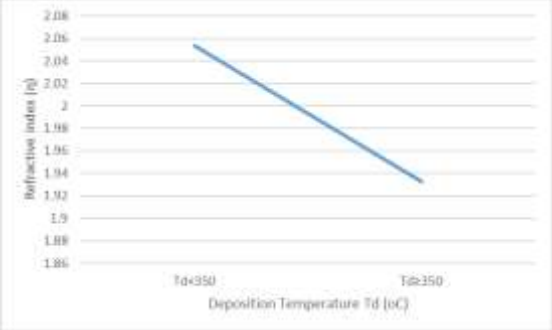

Fig. 12. Refractive index plot against deposition temperature of aged NiO films

Fig. 12 shows the refractive index of the NiO films. The refractive index of deposited films was calculated using refractive index and optical band gap expression as shown in Equation 6 [61]:

$$\eta = \sqrt{(12.417 \,/\, (Eg - 0.365))} \quad (6)$$

Where η denotes refractive index while E_g represents optical band gap.

Refractive indices were found to be 2.0533 and 1.9324 for T_d < 350 ºC and T_d≥350 ºC respectively. This is an improvement on reported values of 1.99 by Sriram and Thayumanavan [32].

4. Conclusion

This study reported spray pyrolysis deposition of aged nanostructured NiO films on glass substrate. The influence of deposition temperature on aged NiO films on elemental, morphological, structural and optical properties was studied with a view to optimizing deposition temperature for solar cell application.

This study contributed new results relating to surface morphology, structural, film thickness and optical of NiO films using spray pyrolysis.

Deposition temperature only affected the surface morphology of aged NiO films by producing a grainier surface. It does not affect the shape and size. Elemental composition using EDX confirmed the presence of Ni and O elements in NiO films. It was observed that the film thickness grew as deposition temperature increased.

NiO films are formed with a non-stoichiometric ratio at lower deposition temperatures, but are electrostatically neutral at higher deposition temperatures.

Transmittance grew from 70.70 % to 76.41 % as deposition temperature increased. This resulted in a reduction in the refractive index of the aged NiO films as deposition temperatures increased. Optical band gap varied from 3.31 eV to 3.69 eV as deposition temperature increased. This study produced better optical band gaps than existing reported values. The new findings were a result of well optimized deposition parameters. Therefore, deposition temperature does affect the properties of aged nanostructured NiO thin films. This optimized result may be explored further for affordable, durable and efficient solar cell fabrication and research in developing countries by ageing the precursor for longer period and at different concentrations, it can also be doped with another material or this result used directly to fabricate a solar device using a pn heterojunction technology. This optimized results will help in affordable and sustainable solar cells fabrication as it will be useful as p-type material in a pn heterojunction solar cells

Acknowledgements

The authors acknowledge the National Research Foundation (NRF) and the World Academy of Science (NRF/TWAS) under grant number 105492 towards this research.

References

[1] M. Grätzel, Mesoscopic solar cells for electricity and hydrogen production from sunlight, Chem. Lett. 34 (2004) 8-13.

[2] C-W. Shyu, Ensuring access to electricity and minimum basic electricity needs as a goal for the post-MDG development agenda after 2015, Energy Sustainable Dev. 19 (2014) 29-38.

[3] R. Adib, Renewables 2015 Global Status Report, Paris: REN21 Secretariat, 2015.

[4] N. Emodi, S. Yusuf, Improving electricity access in Nigeria: obstacles and the way forward, Int. J. Energy Econ. Policy, 5 (2015) 335-351.

[5] O. Henni, M. Belarbi, K. Haddouche, K., & E.H. Belarbi, Design and Implementation of a Low-Cost Characterization System for Photovoltaic Solar Panels, Int. J. of Renew Energy Res, Vol. 7, No. 4, pp. 1586-1594, 2017

[6] C. Chukwuka, K.A. Folly, "Technical and economic modeling of the 2.5kW grid-tie residential photovoltaic system". Int J Renew Energy Res, Vol. 3, No. 2, pp. 412–419, 2013

[7] J. Liu, R. Hou, "Solar cell simulation model for photovoltaic power generation system". Int J Renew Energy Res, Vol. 4, No. 1, pp. 49–53, 2014.

[8] M. Eslamian, Spray-on thin film PV solar cells: advances, potentials and challenges, Coatings, 4 (2014) 60-84.

[9] A.K. Hussein, Applications of nanotechnology in renewable energies: a comprehensive overview and understanding, Renewable Sustainable Energy Rev. 42 (2015) 460-476.

[10] M.T. Ahmed, T. Gonçalves and M. Tlemcani, "Single diode model parameters analysis of photovoltaic cell", ICRERA'2016 5th International Conference on Renewable Energy Research and Applications, Birmingham, UK, pp. 396–400, 20–23 November 2016. (Conference Paper)

[11] M.R. Rashel, A. Albino, M. Tlemcani, T Gonçalves and J. Rifath, "MATLAB Simulink modeling of photovoltaic cells for understanding shadow effect", ICRERA'2016 5th International Conference on Renewable Energy Research and Applications, Birmingham, UK, pp. 747–750, 20–23 November 2016. (Conference Paper)

[12] A. Cordeiro, D. Foito and V. Fernão Pires, "A PV panel simulator based on a two quadrant DC/DC power converter with a sliding mode controller", ICRERA'2015 4th International Conference on Renewable Energy Research and Applications, Palermo, Italy, pp. 928–932, 22–25 November 2015. (Conference Paper)

[13] J. Cubas, S. Pindado and A. Farrahi, "New method for analytical photovoltaic parameter extraction", ICRERA'2013 2nd International Conference on Renewable Energy Research and Applications, Madrid, Spain, pp. 873–877, 20–23 October 2013. (Conference Paper)

[14] A. Parisi, L. Curcio, V. Rocca, S. Stivala and A.C. Cino et al., "Photovoltaic module characteristics from CIGS solar cell modelling", ICRERA'2013 2nd International Conference on Renewable Energy Research and Applications, Madrid, Spain, pp. 1139–1144, 20–23 October 2013. (Conference Paper)

[15] A.S. Islam, M. Islam, Status of renewable energy technologies in Bangladesh, Technol. 5 (2005) 1-5.

[16] C. Eberspacher, C. Fredric, K. Pauls, J. Serra, Thin-film CIS alloy PV materials fabricated using non-vacuum, particles-based techniques, Thin Solid Films, 387 (2001) 18-22.

[17] W. Wang, Y-W. Su, C-H. Chang. Inkjet printed chalcopyrite CuIn x Ga 1− x Se 2 thin film solar cells, Sol. Energy Mater. Sol. Cells, 95 (2011) 2616-2620.

[18] E. Serrano, G. Rus, J. Garcia-Martinez, Nanotechnology for sustainable energy, Renewable Sustainable Energy Rev. 13 (2009) 2373-2384.

[19] W.J. Nam, Z. Gray, J. Stayancho, V. Plotnikov, D. Kwon, S. Waggoner, et al., ALD NiO Thin films as a hole transport-electron blocking layer material for photo-detector and solar cell devices, ECS Transac. 66 (2015) 275-279.

[20] N. Park, K. Sun, Z. Sun, Y. Jing, D. Wang, High efficiency NiO/ZnO heterojunction UV photodiode by sol-gel processing, J. Mater. Chem. C, 1 (2013) 7333-7338.

[21] C. Li, Z. Zhao, Preparation and characterization of nickel oxide thin films by a simple two-step method, Vacuum Electron Sources Conference and Nanocarbon (IVESC), 2010 8th International: IEEE, (2010) 648-649.

[22] C-C. Wu, C-F. Yang, Effect of annealing temperature on the characteristics of the modified spray deposited Li-doped NiO films and their applications in transparent heterojunction diode, Sol. Energy Mater. Sol. Cells, 132 (2015) 492-498.

[23] Z. Zhu, Y. Bai, T. Zhang, Z. Liu, X. Long, Z. Wei, et al., High-Performance hole-extraction layer of sol-gel-processed NiO nanocrystals for inverted planar perovskite solar cells, Angewandte Chemie, 126 (2014) 12779-12783.

[24] C.R. Magaña, D.R. Acosta, A.I. Martínez, J.M. Ortega, Electrochemically induced electrochromic properties in nickel thin films deposited by DC magnetron sputtering, Sol. Energy, 161 (2006) 161-169.

[25] J. Keraudy, J. García Molleja, A. Ferrec, B. Corraze, M. Richard-Plouet, A. Goullet, et al., Structural, morphological and electrical properties of nickel oxide thin films deposited by reactive sputtering, Appl. Surf. Sci. 357 (2015) Part A 838-844.

[26] M. Jlassi, I. Sta, M. Hajji, H. Ezzaouia, Optical and electrical properties of nickel oxide thin films synthesized by sol-gel spin coating, Mater. Sci. Semicon. Processing, 21 (2014) 7-13.

[27] H. Wang, Y. Wang, X. Wang, Pulsed laser deposition of the porous nickel oxide thin film at room temperature for high- rate pseudocapacitive energy storage, Electrochem. Commun. 18 (2012) 92-95.

[28] M.M. El-Nahass, M. Emam-Ismail, M. El-Hagary, Structural, optical and dispersion energy parameters of nickel oxide nanocrystalline thin films prepared by electron beam deposition technique, J. Alloys Compd. 646 (2015) 937-945.

[29] M.A. Vidales-Hurtado, A. Mendoza-Galván, Electrochromism in nickel oxide-based thin films obtained by chemical bath deposition, Solid State Ionics, 179 (2008) 2065-2068.

[30] R. Sharma, A. Acharya, S. Moghe, S. Shrivastava, V. Ganesan, S. Bhardwaj, et al., Effect of deposition temperature on structural and optical properties of sprayed nickel oxide thin films, AIP Conference Proceedings: AIP, (2013) 507-508.

[31] I Fasaki, A. Koutoulaki, M. Kompitsas, C. Charitidis, Structural, electrical and mechanical properties of NiO thin films grown by pulsed laser deposition, Appl. Surf. Sci. 257 (2010) 429-433.

[32] S. Sriram, A. Thayumanavan, Structural, optical and electrical properties of NiO thin films prepared by low cost spray pyrolysis technique, Int. J. Mater. Sci. Eng. 1 (2013) 118-121.

[33] D-M. Na, L. Satyanarayana, G-P. Choi, Y-J. Shin, J.S. Park, Surface morphology and sensing property of NiO-WO3 thin films prepared by thermal evaporation, Sensors, 5 (2005) 519-528.

[34] M.D. Irwin, D.B. Buchholz, A.W. Hains, R.P. Chang, T.J. Marks, p-Type semiconducting nickel oxide as an efficiency-enhancing anode interfacial layer in polymer bulk-heterojunction solar cells, Proc. Natl. Acad. Sci. 105 (2008) 2783-2787.

[35] M. El-Kemary, N. Nagy, I. El-Mehasseb, Nickel oxide nanoparticles: synthesis and spectral studies of interactions with glucose, Mater. Sci. Semicon, Processing, 16 (2013) 1747-1452.

[36] J.C. De Jesus, I. González, A. Quevedo, T Puerta, Thermal decomposition of nickel acetate tetrahydrate: an integrated study by TGA, QMS and XPS techniques, J. Mol. Catal. A: Chem. 228 (2005) 283-291.

[37] H-L. Chen, Y-M. Lu, J-Y. Wu, W-S. Hwang, Effects of substrate temperature and oxygen pressure on crystallographic orientations of sputtered nickel oxide films, Mater. Transac. 46 (2005) 2530-2535.

[38] Y. Lu, W-S. Hwang, J. Yang, Effects of substrate temperature on the resistivity of non-stoichiometric sputtered NiO x films, Surf. Coat. Technol. 155 (2002) 231-235.

[39] B.H.W.S. de Jong, Glass, fifth ed., Weinheim, Germany, VCH, 1989.

[40] M. Gabal, Non-isothermal decomposition of NiC 2 O 4–FeC 2 O 4 mixture aiming at the production of NiFe 2 O 4, J. Phys. Chem. Solids, 64 (2003) 1375-1385.

[41] E. Fujii, A. Tomozawa, H. Torii, R. Takayama, Preferred orientations of NiO films prepared by plasma-enhanced metalorganic chemical vapor deposition, Jpn. J. Appl. Phys. 35 (1996) L328.

[42] H.L. Chen, Y.S. Yang, Effect of crystallographic orientations on electrical properties of sputter-deposited nickel oxide thin films, Thin Solid Films, 516 (2008) 5590-5596.

[43] C.A. Fisher, Molecular dynamics simulations of reconstructed NiO surfaces, Scripta Materialia, 50 (2004) 1045-1049.

[44] P. Scherrer, G. Nachr, Derivation of crystallite size OH HO OH OH OH O OH. 1918.

[45] C. Barrett, T. Massalski, Structure of metals, Oxford, Pergamon Press, 1980.

[46] P. Godse, R. Sakhare, S. Pawar, M. Chougule, S. Sen, P. Joshi, et al., Effect of annealing on structural, morphological, electrical and optical studies of nickel oxide thin films, J. Surf. Eng. Mater. Adv. Technol. 1 (2011) 35.

[47] K. Anandan, V. Rajendran, Morphological and size effects of NiO nanoparticles via solvothermal process and their optical properties, Mater. Sci. Semicon. Processing, 14 (2011) 43-47.

[48] P.L. Geissler, C. Dellago, D. Chandler, J. Hutter, M. Parrinello, Autoionization in liquid water, Science, 291 (2001) 2121-2124.

[49] T. Theivasanthi, M. Alagar, Chemical capping synthesis of nickel oxide nanoparticles and their characterizations studies, arXiv preprint arXiv, (2012) 12124595

[50] H. Qiao, Z. Wei, H. Yang, L. Zhu, X. Yan, Preparation and characterization of NiO nanoparticles by anodic arc plasma method, J. Nanomater. (2009) 5.

[51] A. Balu, V. Nagarethinam, N. Arunkumar, M. Suganya, Nanocrystalline NiO thin films prepared by a low cost simplified spray technique using perfume atomizer, J. Electron. Devices, 13 (2012) 920-930.

[52] R.A. Ismail, S.A. Ghafori, G.A. Kadhim, Preparation and characterization of nanostructured nickel oxide

thin films by spray pyrolysis, Appl. Nanosci. 3 (2013) 509-514.

[53] J. Barman, K. Sarma, M. Sarma, K. Sarma, Structural and optical studies of chemically prepared CdS nanocrystalline thin films, Indian J. Pure Appl. Phys. 46 (2008) 339-343.

[54] F. Ezema, A.. Ekwealor, R Osuji, Effect of thermal annealing on the band GAP and optical properties of chemical bath deposited ZnSe thin films, Turk. J. Phys. 30,pp 157-163, 2006.

[55] V. Estrella, M. Nair, P. Nair, Semiconducting Cu3BiS3 thin films formed by the solid-state reaction of CuS and bismuth thin films, Semicon. Sci. Technol. 18 (2003) 190.

[56] E. Burstein, Anomalous optical absorption limit in InSb, Phys. Rev. 93 (1954) 632.

[57] T. Moss, The interpretation of the properties of indium antimonide, Proc.Phys. Soc. Sect. B, 67 (1954) 775.

[58] G. Boschloo, A. Hagfeldt, Spectroelectrochemistry of nanostructured NiO, J. Phys. Chem. B, 105 (2001) 3039-3044.

[59] S. Makhlouf, M. Kassem, M. Abedulrahim, Crystallite size dependent optical properties of nanostructured NiO films, J. Optoelectron Adv. Mater. 4 (2010) 1562.

[60] R. Romero, F. Martin, J. Ramos-Barrado, D. Leinen, Synthesis and characterization of nanostructured nickel oxide thin films prepared with chemical spray pyrolysis, Thin Solid Films, 518 (2010) 4499-4502.

[61] R. Reddy, Y.N. Aharnmed, P.A. Azeem, K.R. Gopal, B.S. Devi, T. Rao, Dependence of physical parameters of compound semiconductors on refractive index, Defence Sci. J. 53 (2003) 239.